

Advanced Surface Acoustic Wave Resonators on LiTaO₃/SiO₂/Sapphire Substrate

Jinbo Wu^{ID}, *Student Member, IEEE*, Shibin Zhang^{ID}, *Member, IEEE*, Yang Chen, Pengcheng Zheng, *Student Member, IEEE*, Liping Zhang^{ID}, *Student Member, IEEE*, Hulin Yao, Zhongxu Li, Xiaomeng Zhao, Kai Huang, Tao Wu^{ID}, *Senior Member, IEEE*, and Xin Ou^{ID}, *Member, IEEE*

Abstract—The shear horizontal surface acoustic wave (SH-SAW) resonators with excellent quality factor and temperature stability were fabricated on 42°YX-LiTaO₃/SiO₂/sapphire substrate. For comparison, the 4-inch LiTaO₃/SiO₂/sapphire (fully insulating LiTaO₃-on-insulator, FI-LTOI) and LiTaO₃/SiO₂/poly-Si/Si (trap-rich layer assisted LiTaO₃-on-insulator, TR-LTOI) substrates are prepared by ion-cutting process. The GHz acoustic delay lines (ADLs) built on FI-LTOI exhibit a propagation loss of only 2.95 dB/mm, which is 37.5% smaller than the 4.72 dB/mm of the ADLs on TR-LTOI. The demonstrated SH-SAW resonators on FI-LTOI exhibit higher Q -values than those on TR-LTOI. Among them, a FI-LTOI based resonator

with the resonant frequency of 1.76 GHz exhibits a maximum Bode- Q (Q_{\max}) of 4,421, an effective electromechanical coupling coefficient of 13.34%, an excellent figure of merit of 589.8, and a well-compensated temperature coefficient of frequency of -9.1 ppm/°C. More importantly, the Q_{\max} of the FI-LTOI based resonator is maintained well (2,791) even at 200 °C whereas that of the TR-LTOI based resonator decreased to 674. Overall, the FI-LTOI substrate may serve as an advanced material platform of SAW devices for 5G-FR1 bands.

Index Terms—Surface acoustic wave resonator, LiTaO₃-on-insulator, parasitic surface conduction, RF loss, shear horizontal mode, temperature coefficient of frequency.

Manuscript received 19 July 2022; revised 9 August 2022; accepted 17 August 2022. Date of publication 19 August 2022; date of current version 27 September 2022. This work was supported in part by the National Key Research and Development Program of China under Grant 2020YFB2008802 and Grant 2019YFB1803903; in part by the Shanghai Post-Doctoral Excellence Program under Grant 2020487; in part by the Fellowship of China Postdoctoral Science Foundation under Grant 2021M703339; in part by the National Natural Science Foundation of China under Grant 61874128, Grant 11705262, and Grant 61874073; in part by the Frontier Science Key Program of the Chinese Academy of Sciences (CAS) under Grant QYZDY-SSW-JSC032 and Grant ZDBS-LY-JSC009; in part by the Chinese-Austrian Cooperative Research and Development Project under Grant GJHZ201950; in part by the Program of Shanghai Academic Research Leader under Grant 19XD1404600; and in part by the K. C. Wong Education Foundation under Grant GJTD-2019-11. The review of this letter was arranged by Editor N. Barniol. (Jinbo Wu, Shibin Zhang, and Yang Chen contributed equally to this work.) (Corresponding authors: Shibin Zhang; Xin Ou.)

Jinbo Wu is with the State Key Laboratory of Functional Materials for Informatics, Shanghai Institute of Microsystem and Information Technology, Shanghai 200050, China, also with the Center of Materials Science and Optoelectronics Engineering, University of Chinese Academy of Sciences, Beijing 100049, China, and also with the School of Information Science and Technology (SIST), ShanghaiTech University, Shanghai 201210, China.

Shibin Zhang, Xiaomeng Zhao, and Kai Huang are with the State Key Laboratory of Functional Materials for Informatics, Shanghai Institute of Microsystem and Information Technology, Chinese Academy of Sciences, Shanghai 200050, China (e-mail: sbzhang@mail.sim.ac.cn).

Yang Chen, Pengcheng Zheng, Liping Zhang, Hulin Yao, Zhongxu Li, and Xin Ou are with the State Key Laboratory of Functional Materials for Informatics, Shanghai Institute of Microsystem and Information Technology, Chinese Academy of Sciences, Shanghai 200050, China, and also with the Center of Materials Science and Optoelectronics Engineering, University of Chinese Academy of Sciences, Beijing 100049, China (e-mail: ouxin@mail.sim.ac.cn).

Tao Wu is with the School of Information Science and Technology (SIST), ShanghaiTech University, Shanghai 201210, China.

Color versions of one or more figures in this letter are available at <https://doi.org/10.1109/LED.2022.3200418>.

Digital Object Identifier 10.1109/LED.2022.3200418

I. INTRODUCTION

SURFACE acoustic wave (SAW) devices have been extensively used for radio frequency (RF) signal processing in modern wireless communication systems [1], [2], [3], [4], [5], [6], [7] due to their high performance, small size and simple fabrication process. Increasingly crowded frequency bands and denser RF modules require filter elements with steep skirts, low insertion loss (IL) and stable temperature characteristics, which place higher requirements on the quality factor and temperature stability of SAW resonators. Conventional SAWs based on homogeneous piezoelectric crystals (e.g., LiTaO₃ crystal, as schematically shown in Fig. 1(a)) cannot satisfy the increased demands of high-performance filter due to the limited Q -value and poor temperature coefficient of frequency (TCF).

In recent years, piezoelectric films combined with SiO₂ layers (e.g., LiTaO₃/SiO₂, LiNbO₃/SiO₂) [5], [6], [7], [8], [9] have attracted much attentions due to the benefits of tuning TCF, enhancing acoustic energy confinement, suppressing spurious modes, and improving electromechanical coupling coefficients. SAW resonators with LiTaO₃/SiO₂ bi-layer on Si support substrate (LiTaO₃-on-insulator, LTOI, as schematically shown in Fig. 1(b)) [2], [8], [10], [11] have achieved an excellent Bode- Q [12] of 4,000. However, the interface between the SiO₂ dielectric layer and the semiconductor support substrate is prone to the parasitic surface conduction (PSC) effect [13], [14], [15], [16], [17], [18], resulting in increased RF-loss and decreased Q -value. Introducing a trap-rich layer (e.g., poly-Si) [13], [19], removing the semiconductor support substrate [20], [21], [22], [23], [24] and

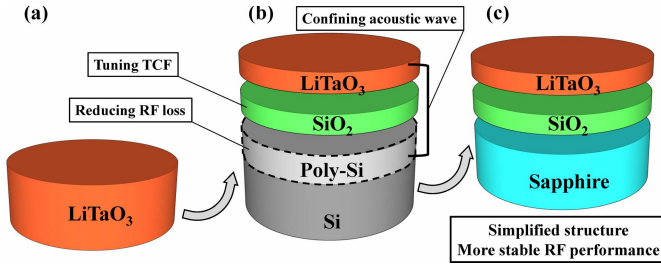


Fig. 1. Schematics of (a) LiTaO₃, (b) LTOI/TR-LTOI, (c) FI-LTOI.

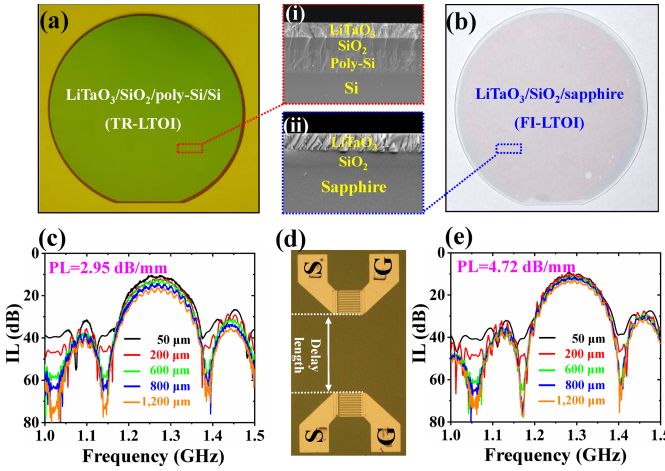


Fig. 2. Photos of the fabricated (a) TR-LTOI and (b) FI-LTOI wafers. (c) Measured and extracted insertion loss of the TR-LTOI ADLs. (d) The optical microscope image of a fabricated ADL. (e) Measured insertion loss of the FI-LTOI ADLs. The cross-sectional SEM images of the (i) TR-LTOI and (ii) FI-LTOI substrates.

adopting the insulator support substrate [24], [25], [26] are effective methods to eliminate the PSC effect. For example, SAW resonators on LiTaO₃/SiO₂/poly-Si/Si substrates (trap-rich layer assisted LiTaO₃-on-insulator, TR-LTOI, as schematically shown in Fig. 1(b)) [3], [19] have achieved a high Q_{\max} of about 6,000 due to the reduced RF loss. However, the multi-layer structures result in relatively complex and expensive fabrication processes.

In this work, the LiTaO₃/SiO₂/sapphire substrate (fully insulating LiTaO₃-on-insulator, FI-LTOI, as schematically shown in Fig. 1(c)) have been proposed as a novel material platform for SAW devices. The 4-inch FI-LTOI and TR-LTOI substrates were prepared by ion-cutting process [27]. Acoustic delay lines (ADLs) built on FI-LTOI show much lower propagation loss than those built on TR-LTOI, while SH-SAW resonators built on FI-LTOI exhibit higher Q -values than those on TR-LTOI. In addition, at the ambient temperature of 200 °C, the Q_{\max} of TR-LTOI based resonator decreases to less than 20% of that at 25 °C, while that of the FI-LTOI based resonator still maintained quite high.

II. SUBSTRATE LOSS OF TR-LTOI AND FI-LTOI

The 4-inch single-crystalline 42°YX-LiTaO₃ thin films were transferred onto both the SiO₂/sapphire substrate and the SiO₂/poly-Si/Si substrate by ion-cutting process under the same conditions for comparison. Figs. 2(a) and (b) show the photos of the two wafers, while the insets show the

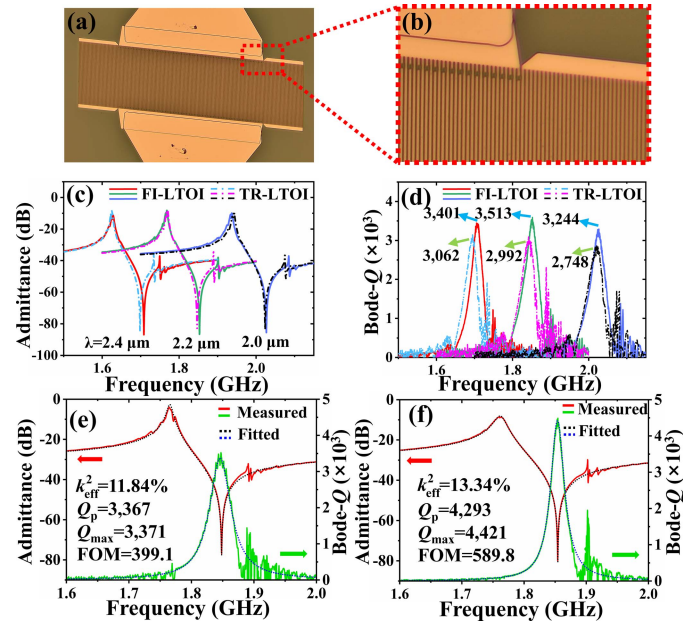


Fig. 3. (a) The optical microscope image (top view) and the (b) zoomed-in image of a fabricated resonator. Measured (c) admittance curves and (d) Bode- Q curves of the FI-LTOI based (solid) and TR-LTOI based (dot) resonators. Measured (solid) and fitted (dot) frequency responses of the (e) TR-LTOI based and (f) FI-LTOI based SAW resonators.

corresponding cross-sectional SEM images. The thickness of the LiTaO₃ films in TR-LTOI and FI-LTOI are around 580 nm \pm 20 nm, respectively, and the thickness of SiO₂ is 500 nm in both substrates.

To evaluate the substrate loss, the ADLs with different delay length were built on the two substrates. Fig. 2(d) shows the optical microscope image of a fabricated ADL. The measured insertion loss (IL) of the ADLs with $\lambda = 3.2 \mu\text{m}$ on the TR-LTOI and FI-LTOI substrates are shown in Figs. 2(c) and (e), respectively. Thanks to the excellent insulating properties of the sapphire support substrate, the extracted propagation loss (PL) of the FI-LTOI substrate is only 2.95 dB/mm, which is 37.5% smaller than the 4.72 dB/mm of the TR-LTOI substrate. Comparing FI-LTOI based ADLs with some other solid mounted ADLs [25], [28], [29], FI-LTOI based ADLs achieve the smallest PL so far. Note that the smaller PL corresponds to higher equivalent Q -values of substrates [30], [31]. It is seen that the substrate loss of the SH-SAW devices can be significantly reduced by the insulating sapphire substrate, and SAW devices with higher Q -values may be achieved.

III. HIGH PERFORMANCE FI-LTOI SAW RESONATORS

SH-SAW resonators were fabricated using electron-beam lithography, metal evaporation, and the lift-off process. The metal consists of Ti/Al/Ti with thicknesses of 2 nm, 120 nm and 2 nm, respectively. The optical microscope image and the zoomed-in image of a fabricated SH-SAW resonator are shown in Figs. 3(a) and (b), respectively. Tilted resonators [10] are used here to suppress the transverse spurious modes.

The frequency responses of the fabricated SAW devices were characterized using a vector network analyzer (Keysight E5071C) with a terminal impedance of 50 Ω

TABLE I
COMPARISON OF SH-SAW RESONATORS

Ref.	substrate	f_s (GHz)	Q_{\max}	k_{eff}^2 (%)	FOM
[8]	LiTaO ₃ /SiO ₂ /Si	1.9	4,000	9.8	392
[2]	LiTaO ₃ /SiO ₂ /AlN/Si	1.9	4,200	9.8	411.6
[19]	LiTaO ₃ /SiO ₂ / poly-Si/Si	1.53	~6,000	11.9	714
[6]	LiNbO ₃ /SiO ₂ /Si	~1.1	388	~32.1	124.5
[26]	LiTaO ₃ /sapphire	1.76	3019	5.14	155
	LiTaO ₃ /SiO ₂ / poly-Si/Si	1.76	3,371	11.84	399.1
This work	LiTaO ₃ /SiO ₂ /sapphire	1.76	4,421	13.34	589.8

at room temperature in air. Fig. 3(c) shows the measured admittance curves of the FI-LTOI based and TR-LTOI based resonators with different electrode periodicities (λ) of 2.0~2.4 μm . The aperture length of the above resonators is 20λ . Fig. 3(d) shows the corresponding Bode- Q curves, where the extracted Q_{\max} values of the FI-LTOI based resonators are 11%~18% higher than those of TR-LTOI based resonators. For a more detailed comparison, Figs. 3(e) and (f) show the measured and fitted frequency responses of two resonators with the same design ($\lambda = 2.2 \mu\text{m}$ and aperture length of 40λ) on both substrates. The FI-LTOI based resonator exhibits an excellent Q_{\max} up to 4,421, which is 31.1% larger than the 3,371 of the TR-LTOI based one. Besides, FI-LTOI based resonator shows a k_{eff}^2 [32] of 13.34% and an outstanding figure of merit ($\text{FoM} = k_{\text{eff}}^2 \times Q_{\max}$) of 589.8, which is 47.8% larger than that of the TR-LTOI based one. In a word, the SH-SAW devices on the FI-LTOI substrate achieve higher performance with a simpler substrate structure.

A comparison between this work and some other SH-SAW resonators with different substrates [2], [8], [6], [19], [26] is shown in Table I. The FI-LTOI based resonator in this work shows a quite high Q_{\max} and FoM, which are very close to the state-of-the-art [19]. It is worth noting that the k_{eff}^2 and Q -values of the FI-LTOI based resonator in this work are significantly improved compared to the previous work (SAW devices based on the LiTaO₃/sapphire substrate [26]). The optimized substrate preparation process minimizes the ion implantation-induced damages, thereby improving the k_{eff}^2 and reducing the intrinsic loss of the material. The introduction of the SiO₂ low acoustic velocity layer enhances the confinement of the acoustic energy in the thickness direction, while reducing the in-plane diffraction by changing the in-plane anisotropy [10], [33]. Besides, the introduced SiO₂ layer also increases the k_{eff}^2 in this work due to the smaller stiffness coefficient and dielectric constant of SiO₂ [34]. Both the optimized substrate preparation process and the introduced SiO₂ layer contribute to the improvements, and higher Q_{\max} can be expected by further optimizing the device design and reducing the ohmic losses of the electrodes.

IV. TEMPERATURE CHARACTERISTICS OF FI-LTOI SAW

To investigate the temperature stability, the resonators demonstrated on both substrates were tested in the temperature range of ~25–200 °C, and Figs. 4(a) and (b) show the measured and zoomed-in admittance curves. The fitted first-order temperature coefficient of frequency (TCF) at resonant

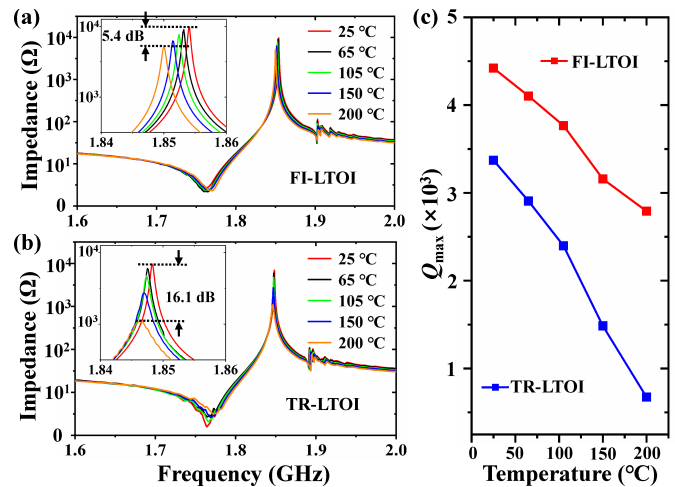


Fig. 4. Measured and zoomed-in admittance curves of (a) TR-LTOI SAW and (b) FI-LTOI SAW resonators in the temperature range of ~25–200 °C. (c) Variation of Q_{\max} with temperature for TR-LTOI SAW and FI-LTOI SAW resonators.

(f_r) and anti-resonant frequencies (f_a) of the FI-LTOI based resonator are 11.3 ppm/°C and -9.1 ppm/°C, respectively. Such a resonator with small TCFs at both the f_r and f_a is very promising for frequency-sensitive filters. More importantly, the impedance attenuation of the FI-LTOI based resonator (at f_a) is only 5.4 dB at 200 °C whereas that of the TR-LTOI based resonator reaches 16.1 dB. Fig. 4(c) shows the extracted Q_{\max} values of resonators on both substrates at different temperatures. When the temperature increases, the effective resistivity at the SiO₂/Si interface will gradually decrease, while that at the SiO₂/sapphire interface is still large enough due to the excellent insulating properties of sapphire. Therefore, the SH-SAW devices on FI-LTOI achieve better RF performance over the temperature range of 25 to 200 °C than those on TR-LTOI. At 200 °C, the Q_{\max} of the FI-LTOI based resonator still reaches 2,791 whereas that of TR-LTOI based one decreases to 674.

V. CONCLUSION

In this work, the FI-LTOI and TR-LTOI substrates were fabricated by ion-cutting process under the same conditions. The presence of the excellent insulating sapphire substrate helps the FI-LTOI substrate to obtain lower propagation loss, and therefore better Q of the SAW devices. The SH-SAW resonator built on the FI-LTOI substrate shows an excellent Q_{\max} of 4,421, a k_{eff}^2 of 13.34%, a FoM of 589.8, and the well-compensated TCFs of 11.3 ppm/°C and -9.1 ppm/°C at f_r and f_a , respectively. Most importantly, even at 200 °C, the Q -values of the FI-LTOI based resonators are still well maintained while those of the TR-LTOI based resonators are severely attenuated. Overall, those results in this work demonstrate the great potential of SAW devices on FI-LTOI substrates for low-loss and temperature-sensitive applications in RF wireless communications.

ACKNOWLEDGMENT

The authors would like to thank the Fudan Nano-fabrication Laboratory and the ShanghaiTech Quantum Device Laboratory (SQDL) for device fabrication support.

REFERENCES

- [1] K.-Y. Hashimoto, M. Kadota, T. Nakao, M. Ueda, M. Miura, H. Nakamura, H. Nakanishi, and K. Suzuki, "Recent development of temperature compensated SAW devices," in *Proc. IEEE Int. Ultrason. Symp.*, Oct. 2011, pp. 79–86, doi: [10.1109/ULTSYM.2011.0021](https://doi.org/10.1109/ULTSYM.2011.0021).
- [2] T. Takai, H. Iwamoto, Y. Takamine, H. Yamazaki, T. Fuyutsume, H. Kyoya, T. Nakao, H. Kando, M. Hiramoto, T. Toi, M. Koshino, and N. Nakajima, "High-performance SAW resonator on new multi-layered substrate using LiTaO₃ crystal," *IEEE Trans. Ultrason., Ferroelectr., Freq. Control*, vol. 64, no. 9, pp. 1382–1389, Sep. 2017, doi: [10.1109/TUFFC.2017.2738119](https://doi.org/10.1109/TUFFC.2017.2738119).
- [3] E. Butaud, B. Tavel, S. Ballandras, M. Bousquet, A. Drouin, I. Huyet, E. Courjon, A. Ghorbel, A. Reinhardt, A. Clairet, F. Bernard, and I. Bertrand, "Smart cutTM piezo on insulator (POI) substrates for high performances SAW components," in *Proc. IEEE Int. Ultrason. Symp. (IUS)*, Sep. 2020, pp. 1–4, doi: [10.1109/IUS46767.2020.9251517](https://doi.org/10.1109/IUS46767.2020.9251517).
- [4] S. Zhang, R. Lu, H. Zhou, S. Link, Y. Yang, Z. Li, K. Huang, X. Ou, and S. Gong, "Surface acoustic wave devices using lithium niobate on silicon carbide," *IEEE Trans. Microw. Theory Techn.*, vol. 68, no. 9, pp. 3653–3666, Sep. 2020, doi: [10.1109/TMTT.2020.3006294](https://doi.org/10.1109/TMTT.2020.3006294).
- [5] H. Zhou, S. Zhang, Z. Li, K. Huang, P. Zheng, J. Wu, C. Shen, L. Zhang, T. You, L. Zhang, K. Liu, H. Sun, H. Xu, X. Zhao, and X. Ou, "Surface wave and Lamb wave acoustic devices on heterogenous substrate for 5G front-ends," in *IEDM Tech. Dig.*, Dec. 2020, pp. 17.6.1–17.6.4, doi: [10.1109/IEDM13553.2020.9372128](https://doi.org/10.1109/IEDM13553.2020.9372128).
- [6] R. Su, J. Shen, Z. Lu, H. Xu, Q. Niu, Z. Xu, F. Zeng, C. Song, W. Wang, S. Fu, and F. Pan, "Wideband and low-loss surface acoustic wave filter based on 15° YX-LiNbO₃/SiO₂/Si structure," *IEEE Electron Device Lett.*, vol. 42, no. 3, pp. 438–441, Mar. 2021, doi: [10.1109/LED.2021.3051298](https://doi.org/10.1109/LED.2021.3051298).
- [7] T.-H. Hsu, K.-J. Tseng, and M.-H. Li, "Large coupling acoustic wave resonators based on LiNbO₃/SiO₂/Si functional substrate," *IEEE Electron Device Lett.*, vol. 41, no. 12, pp. 1825–1828, Dec. 2020, doi: [10.1109/LED.2020.3030797](https://doi.org/10.1109/LED.2020.3030797).
- [8] T. Takai, H. Iwamoto, Y. Takamine, T. Fuyutsume, T. Nakao, M. Hiramoto, T. Toi, and M. Koshino, "High-performance SAW resonator with simplified LiTaO₃/SiO₂ double layer structure on Si substrate," *IEEE Trans. Ultrason., Ferroelectr., Freq. Control*, vol. 66, no. 5, pp. 1006–1013, May 2019, doi: [10.1109/TUFFC.2019.2898046](https://doi.org/10.1109/TUFFC.2019.2898046).
- [9] A. Kochhar, A. Mahmoud, Y. Shen, N. Turumella, and G. Piazza, "X-cut lithium niobate-based shear horizontal resonators for radio frequency applications," *J. Microelectromech. Syst.*, vol. 29, no. 6, pp. 1464–1472, Dec. 2020, doi: [10.1109/JMEMS.2020.3026167](https://doi.org/10.1109/JMEMS.2020.3026167).
- [10] H. Iwamoto, T. Takai, Y. Takamine, T. Nakao, T. Fuyutsume, and M. Koshino, "Transverse modes in I.H.P. SAW resonator and their suppression method," in *Proc. IEEE Int. Ultrason. Symp. (IUS)*, Oct. 2018, pp. 1–4, doi: [10.1109/ULTSYM.2018.8580175](https://doi.org/10.1109/ULTSYM.2018.8580175).
- [11] T. Takai, H. Iwamoto, Y. Takamine, H. Yamazaki, T. Fuyutsume, H. Kyoya, T. Nakao, H. Kando, M. Hiramoto, T. Toi, M. Koshino, and N. Nakajima, "Incredible high performance SAW resonator on novel multi-layered substrate," in *Proc. IEEE Int. Ultrason. Symp. (IUS)*, Tours, France, Sep. 2016, pp. 1–4, doi: [10.1109/ULTSYM.2016.7728455](https://doi.org/10.1109/ULTSYM.2016.7728455).
- [12] D. A. Feld, R. Parker, R. Ruby, P. Bradley, and S. Dong, "After 60 years: A new formula for computing quality factor is warranted," in *Proc. IEEE Ultrason. Symp.*, Nov. 2008, pp. 431–436, doi: [10.1109/ULTSYM.2008.0105](https://doi.org/10.1109/ULTSYM.2008.0105).
- [13] C. R. Neve and J.-P. Raskin, "RF harmonic distortion of CPW lines on HR-Si and trap-rich HR-Si substrates," *IEEE Trans. Electron Devices*, vol. 59, no. 4, pp. 924–932, Apr. 2012, doi: [10.1109/TED.2012.2183598](https://doi.org/10.1109/TED.2012.2183598).
- [14] D. Lederer and J.-P. Raskin, "Effective resistivity of fully-processed SOI substrates," *Solid-State Electron.*, vol. 49, no. 3, pp. 491–496, Mar. 2005, doi: [10.1016/j.sse.2004.12.003](https://doi.org/10.1016/j.sse.2004.12.003).
- [15] W. Heinrich, "Quasi-TEM description of MMIC coplanar lines including conductor-loss effects," *IEEE Trans. Microw. Theory Techn.*, vol. 41, no. 1, pp. 45–52, Jan. 1993, doi: [10.1109/22.210228](https://doi.org/10.1109/22.210228).
- [16] H. S. Gamble, B. M. Armstrong, S. J. N. Mitchell, Y. Wu, V. F. Fusco, and J. A. C. Stewart, "Low-loss CPW lines on surface stabilized high-resistivity silicon," *IEEE Microw. Guided Wave Lett.*, vol. 9, no. 10, pp. 395–397, Oct. 1999, doi: [10.1109/75.798027](https://doi.org/10.1109/75.798027).
- [17] D. Lederer and J.-P. Raskin, "New substrate passivation method dedicated to HR SOI wafer fabrication with increased substrate resistivity," *IEEE Electron Device Lett.*, vol. 26, no. 11, pp. 805–807, Nov. 2005, doi: [10.1109/LED.2005.857730](https://doi.org/10.1109/LED.2005.857730).
- [18] Y. Wu, H. S. Gamble, B. M. Armstrong, V. F. Fusco, and J. A. C. Stewart, "SiO₂ interface layer effects on microwave loss of high-resistivity CPW line," *IEEE Microw. Guided Wave Lett.*, vol. 9, no. 1, pp. 10–12, Jan. 1999, doi: [10.1109/75.752108](https://doi.org/10.1109/75.752108).
- [19] E. Butaud, S. Ballandras, M. Bousquet, A. Drouin, B. Tavel, I. Huyet, A. Clairet, I. Bertrand, A. Ghorbel, and A. Reinhardt, "Innovative smart cutTM piezo on insulator (POI) substrates for 5G acoustic filters," in *IEDM Tech. Dig.*, Dec. 2020, pp. 34.6.1–34.6.4, doi: [10.1109/IEDM13553.2020.9372020](https://doi.org/10.1109/IEDM13553.2020.9372020).
- [20] A. Gao and J. Zou, "Extremely high Q AlN Lamb wave resonators implemented by weighted electrodes," in *IEDM Tech. Dig.*, Dec. 2019, pp. 34.5.1–34.5.4, doi: [10.1109/IEDM19573.2019.8993608](https://doi.org/10.1109/IEDM19573.2019.8993608).
- [21] Y. Yang, R. Lu, and S. Gong, "High Q antisymmetric mode lithium niobate MEMS resonators with spurious mitigation," *J. Microelectromech. Syst.*, vol. 29, no. 2, pp. 135–143, Apr. 2020, doi: [10.1109/JMEMS.2020.2967784](https://doi.org/10.1109/JMEMS.2020.2967784).
- [22] T. D. Ha and J. Bao, "Reducing anchor loss in thin-film aluminum nitride-on-diamond contour mode MEMS resonators with support tethers based on phononic crystal strip and reflector," *Microsyst. Technol.*, vol. 22, no. 4, pp. 791–800, Apr. 2016, doi: [10.1007/s00542-015-2678-1](https://doi.org/10.1007/s00542-015-2678-1).
- [23] V. Plessky, S. Yandrapalli, P. J. Turner, L. G. Villanueva, J. Koskela, M. Faizan, A. De Pastina, B. Garcia, J. Costa, and R. B. Hammond, "Laterally excited bulk wave resonators (XBARs) based on thin lithium niobate platelet for 5 GHz and 13 GHz filters," in *IEEE MTT-S Int. Microw. Symp. Dig.*, Jun. 2019, pp. 512–515, doi: [10.1109/MWSYM.2019.8700876](https://doi.org/10.1109/MWSYM.2019.8700876).
- [24] L. Gao, Y. Yang, and S. Gong, "Investigating substrate loss in MEMS acoustic resonators and on-chip inductors," *IEEE Trans. Ultrason., Ferroelectr., Freq. Control*, vol. 69, no. 6, pp. 2178–2189, Jun. 2022, doi: [10.1109/TUFFC.2022.3168539](https://doi.org/10.1109/TUFFC.2022.3168539).
- [25] R. Lu, Y. Yang, A. E. Hassanien, and S. Gong, "Gigahertz low-loss and high power handling acoustic delay lines using thin-film lithium-niobate-on-sapphire," *IEEE Trans. Microw. Theory Techn.*, vol. 69, no. 7, pp. 3246–3254, Jul. 2021, doi: [10.1109/TMTT.2021.3074918](https://doi.org/10.1109/TMTT.2021.3074918).
- [26] J. Wu, S. Zhang, L. Zhang, H. Zhou, P. Zheng, H. Yao, Z. Li, K. Huang, T. Wu, and X. Ou, "Exploring low-loss surface acoustic wave devices on heterogeneous substrates," *IEEE Trans. Ultrason., Ferroelectr., Freq. Control*, vol. 69, no. 8, pp. 2579–2584, Aug. 2022, doi: [10.1109/TUFFC.2022.3179699](https://doi.org/10.1109/TUFFC.2022.3179699).
- [27] Y. Yan, K. Huang, H. Zhou, X. Zhao, W. Li, Z. Li, A. Yi, H. Huang, J. Lin, S. Zhang, M. Zhou, J. Xie, X. Zeng, R. Liu, W. Yu, T. You, and X. Ou, "Wafer-scale fabrication of 42° rotated Y-cut LiTaO₃-on-insulator (LTOI) substrate for a SAW resonator," *ACS Appl. Electron. Mater.*, vol. 1, no. 8, pp. 1660–1666, Aug. 2019, doi: [10.1021/acsaem.9b00351](https://doi.org/10.1021/acsaem.9b00351).
- [28] R. Lu, Y. Yang, A. E. Hassanien, and S. Gong, "Low-loss and high power handling acoustic delay lines using thin-film lithium niobate on sapphire," in *IEEE MTT-S Int. Microw. Symp. Dig.*, Jun. 2021, pp. 270–273, doi: [10.1109/IMS19712.2021.9574829](https://doi.org/10.1109/IMS19712.2021.9574829).
- [29] P. Zheng, S. Zhang, H. Zhou, L. Zhang, J. Wu, H. Yao, K. Huang, X. Zhao, T. You, and X. Ou, "Ultra-low loss and high phase velocity acoustic delay lines in lithium niobate on silicon carbide platform," in *Proc. IEEE 35th Int. Conf. Micro Electro Mech. Syst. Conf. (MEMS)*, Jan. 2022, pp. 1030–1033, doi: [10.1109/MEMS51670.2022.9699566](https://doi.org/10.1109/MEMS51670.2022.9699566).
- [30] R. Lu, Y. Yang, and S. Gong, "Acoustic loss in thin-film lithium niobate: An experimental study," *J. Microelectromech. Syst.*, vol. 30, no. 4, pp. 632–641, Aug. 2021, doi: [10.1109/JMEMS.2021.3092724](https://doi.org/10.1109/JMEMS.2021.3092724).
- [31] R. Lu, Y. Yang, and S. Gong, "Acoustic loss of GHz higher-order Lamb waves in thin-film lithium niobate: A comparative study," *J. Microelectromech. Syst.*, vol. 30, no. 6, pp. 876–884, Dec. 2021, doi: [10.1109/JMEMS.2021.3114627](https://doi.org/10.1109/JMEMS.2021.3114627).
- [32] S. Gong and G. Piazza, "Design and analysis of lithium-niobate-based high electromechanical coupling RF-MEMS resonators for wideband filtering," *IEEE Trans. Microw. Theory Techn.*, vol. 61, no. 1, pp. 403–414, Jan. 2013, doi: [10.1109/TMTT.2012.2228671](https://doi.org/10.1109/TMTT.2012.2228671).
- [33] T. L. Azabo and A. J. Slobodnik, "The effect of diffraction on the design of acoustic surface wave devices," *IEEE Trans. Sonics Ultrason.*, vol. SU-20, no. 3, pp. 240–251, Jul. 1973, doi: [10.1109/T-SU.1973.29751](https://doi.org/10.1109/T-SU.1973.29751).
- [34] S. Inoue and M. Solal, "Spurious free SAW resonators on layered substrate with ultra-high Q, high coupling and small TCF," in *Proc. IEEE Int. Ultrason. Symp. (IUS)*, Oct. 2018, pp. 1–9, doi: [10.1109/ULTSYM.2018.8579852](https://doi.org/10.1109/ULTSYM.2018.8579852).